

AnyBimanual: Transferring Unimanual Policy for General Bimanual Manipulation

Guanxing Lu^{*,1}, Tengbo Yu^{*,1}, Haoyuan Deng², Season Si Chen¹, Yansong Tang^{†,1}, Ziwei Wang²

¹Tsinghua Shenzhen International Graduate School, Tsinghua University

²School of Electrical and Electronic Engineering, Nanyang Technological University

{lgx23@mails., ytb23@mails., season.chen@, tang.yansong@}sz.tsinghua.edu.cn

{E230112@e., ziwei.wang@}ntu.edu.sg

<https://anybimanual.github.io/>

Abstract

Performing general language-conditioned bimanual manipulation tasks is of great importance for many applications ranging from household service to industrial assembly. However, collecting bimanual manipulation data is expensive due to the high-dimensional action space, which poses challenges for conventional methods to handle general bimanual manipulation tasks. In contrast, unimanual policy has recently demonstrated impressive generalizability across a wide range of tasks because of scaled model parameters and training data, which can provide sharable manipulation knowledge for bimanual systems. To this end, we propose a plug-and-play method named **AnyBimanual**, which transfers pretrained unimanual policy to general bimanual manipulation policy with few bimanual demonstrations. Specifically, we first introduce a skill manager to dynamically schedule the skill representations discovered from pretrained unimanual policy for bimanual manipulation tasks, which linearly combines skill primitives with task-oriented compensation to represent the bimanual manipulation instruction. To mitigate the observation discrepancy between unimanual and bimanual systems, we present a visual aligner to generate soft masks for visual embedding of the workspace, which aims to align visual input of unimanual policy model for each arm with those during pre-training stage. **AnyBimanual** shows superiority on 12 simulated tasks from RL Bench2 with a sizable 17.33% improvement in success rate over previous methods. Experiments on 9 real-world tasks further verify its practicality with an average success rate of 84.62%.

1. Introduction

Bimanual systems play an important role in robotic manipulation due to the high capacity of completing diverse tasks

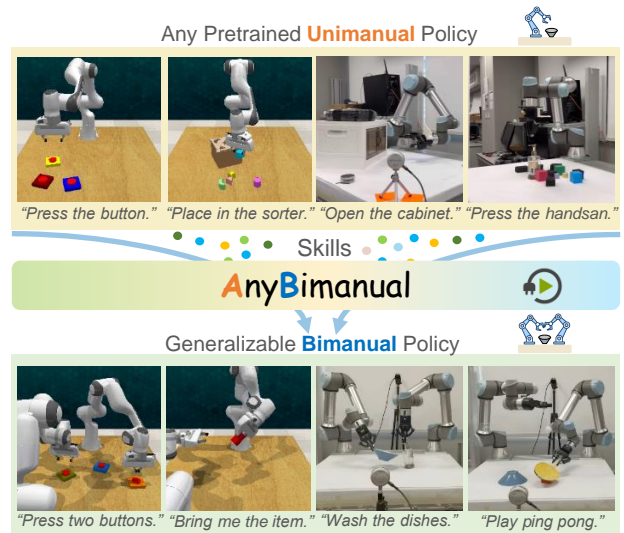


Figure 1. **AnyBimanual** enables plug-and-play transferring from pretrained unimanual policies to bimanual manipulation policy, which preserves the generalizability with the proposed skill scheduling framework.

in household service [72], robotic surgery [33], and component assembly in factories [9]. Compared to unimanual systems, bimanual systems enlarge the workspace and are able to handle more complex manipulation tasks by stabilizing the target with one arm and interacting with that using another arm [30, 45]. Even for the tasks that unimanual policies can handle, bimanual systems are often more efficient because multiple action steps can be simultaneously accomplished [31]. Since modern robotic applications require the robot to interact with different tasks and objects, it is desirable to design a generalizable policy model for bimanual manipulation.

To enhance the generalization ability of the manipula-

tion agent, prior works present to leverage the high-level reasoning and semantic understanding capabilities of foundation models like Large Language Models (LLMs) and Vision Language Models (VLMs) to breakdown tasks into executable sub-tasks that can be solved by external low-level controllers [26, 27, 34, 37, 44], which thus struggles with contact-rich tasks that require complex and precise low-level motion. To generalize to contact-rich tasks, recent methods [1, 41, 51] tend to learn robotic foundation models directly from large-scale teleoperation data [17, 40, 55], which has shown impressive generalizability across various unimanual tasks. However, bimanual demonstrations are extremely expensive to acquire in real-world, which often need specialized teleoperation systems with additional sensors and fine-grained calibration with high human laborer cost [12, 18, 22, 56, 62, 73]. To address this challenge, recent methods aim to simplify the learning budget by exploiting human inductive bias like parameterized atomic movements that detail the position and rotation [5, 15] or assigning stabilizing and acting roles for each arm [24, 45, 54], thereby reducing the need for extensive expert data. Nevertheless, shareable atomic movements and fixed cooperation patterns struggle to generalize across different bimanual manipulation tasks, which limits the deployment scenario of these classes of methods.

In this paper, we propose a plug-and-play module named AnyBimanual that transfers any pre-trained unimanual policy to bimanual manipulation policy with limited demonstrations. Since unimanual policy model [39, 50] has demonstrated impressive generalization ability across tasks due to the large model sizes and numerous training demonstrations, we realize high generalizability across diverse language-conditioned bimanual manipulation tasks by mining and transferring the commonsense knowledge in pre-trained unimanual policies. More specifically, we first introduce a skill manager that dynamically schedules discovered skill representations. Skill representations are formed by skill primitives that store shareable manipulation knowledge across embodiments, with task-oriented importance weights and compensation. To enhance the transferability of the pretrained unimanual policy in bimanual manipulation tasks, the observation discrepancy between unimanual and bimanual systems should be minimized. We propose a voxel aligner to generate spatial soft masks to highlight relevant visual clues for different arms, whose goal is to align the visual input of the unimanual policy model for each arm with those during the pretraining stage. We evaluate AnyBimanual on a comprehensive task suite composed of 12 simulated tasks from RLBench2 [31] and 9 real-world tasks, where our method surpasses the previous state-of-the-art method by a large margin. The contributions are summarized as follows:

- We propose a model-agnostic plug-and-play framework

named AnyBimanual that transfers an arbitrary pretrained unimanual policy to generalizable bimanual manipulation policy with limited bimanual demonstrations.

- We introduce a skill manager to dynamically schedule skill representations for unimanual policy transferring and a visual aligner to mitigate the observation discrepancy between unimanual and bimanual systems for transferability enhancement.
- We conduct extensive experiments of 12 tasks from RLBench2 and 9 tasks from the real world. The results demonstrate that our method achieves a higher success rate than the state-of-the-art methods.

2. Related Work

Generalizable Bimanual Manipulation. Bimanual manipulation agents [6, 11, 22, 24, 27, 31, 38, 45, 68, 71] are able to handle a large variety of tasks by predicting a trajectory of bimanual operation, which is of great significance in complex applications from household service [72], robotic surgery [33], to component assembly in factories [9]. To achieve multi-task learning for generalizable Bimanual manipulation, earlier studies attempted to leverage the emerged general understanding and reasoning capacities of pretrained foundation models like LLMs [53] and VLMs [10], where the foundation model was prompted to generate a high-level plan for low-level executors. However, the performance of directly leveraging foundation models in a training-free manner is bottlenecked by the predefined low-level executor, which struggles to generalize to more contact-rich tasks like straightening a rope. To overcome this challenge, robotic foundation models [7, 8, 17, 41, 46, 51] that pretrained on large-scale real-world demonstrations were proposed under the unimanual setting, which has shown high generalizability across everyday manipulation tasks. However, bimanual tasks demand precise coordination of two high degree-of-freedom arms, making the teleoperation of demonstrations for training generalizable policies also costly. Although some recent approaches [13, 16, 18, 22, 65, 73] have developed more specialized teleoperation systems to reduce these costs, scaling up demonstrations for high generalization ability remains a challenge. To address the limited availability of demonstrations, alternative methods [30, 45, 60] proposed to simplify the learning of bimanual policies by decoupling the bimanual system into a stabilizing arm and an acting arm. Nevertheless, these methods often rely on predefined roles for each arm, which precludes their applicability to tasks requiring more flexible collaboration patterns. In contrast to these approaches, our work presents a novel method that transfers generalizable unimanual policies to bimanual tasks, which eliminates the necessity for explicit inductive bias like role specification.

Skill-based Methods. Skill learning [70] is the process

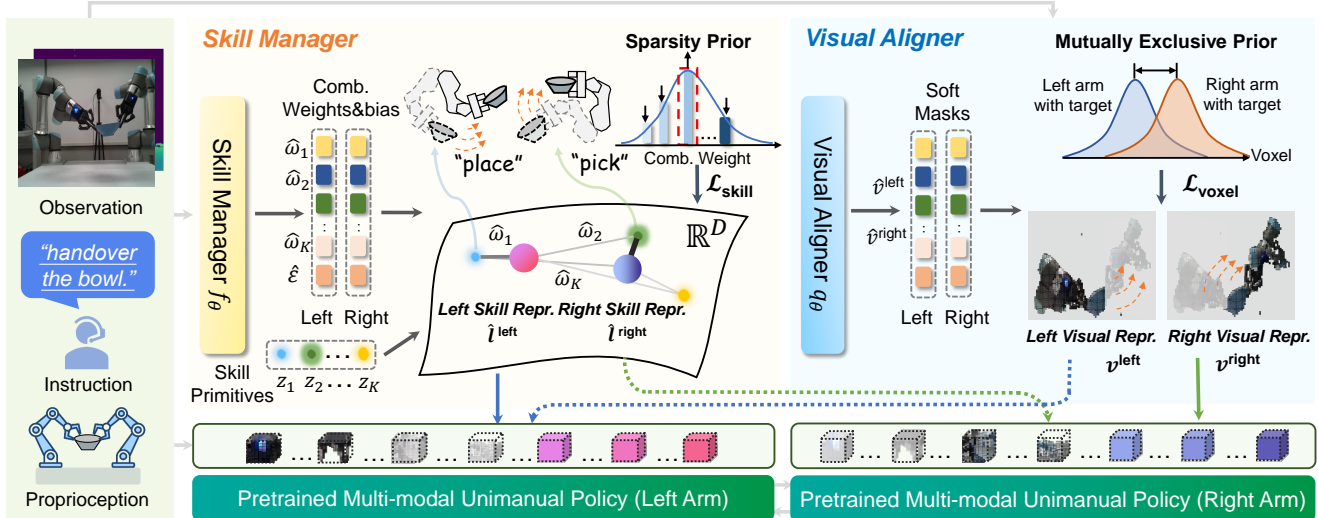


Figure 2. **The overall pipeline of AnyBimanual**, which primarily consists of a skill manager and a perception manager. The skill manager adaptively coordinates primitive skills for each robot arm, while the perception manager mitigates the distributional shift from unimanual to bimanual by decomposing the 3D voxel observation for each arm.

where intelligent agents acquire new abilities that are transferable across different tasks, which is of great significance for cross-task generalization. Thus, skill learning is being attractive in enhancing the generalizability of different models, such as game agents [57], robotic manipulation [43], and autonomous driving [20]. The initial attempt to utilize skill learning was orchestrating a set of predefined skill [48], which hindered their scalability to unseen tasks. To overcome this limitation, [15, 43] proposed to learn shareable skill primitives from data. For example, skill diffuser [43] introduced a hierarchical planning framework that integrates learnable skill embedding into conditional trajectory generation, which realized accurate execution of diverse compositional tasks. In the field of bimanual manipulation, skill learning was dominated by handcrafted primitives. For example, [2–4, 14, 19, 21, 23, 29, 32, 64, 66] propose to utilize parameterized atomic movements to shrink the high dimensionality of the bimanual action space, which has shown impressive performance on templated bimanual manipulation tasks. While the predefined atomic movements did boost the success rate on specific tasks, they are often difficult for even human users to specify, which restricts the deployment scenarios of these methods. In this paper, we propose leveraging learnable skill primitives to represent the learned commonsense of the pretrained unimanual policy, so that the knowledge can be transferred across different levels of tasks.

3. Approach

In this section, we first introduce required preliminaries (Section 3.1), and then we present a pipeline overview (Sec-

tion 3.2). Then, we introduce a skill manager (Section 3.3) that schedules skills to each arm to form general bimanual manipulation policies. We build a visual aligner (Section 3.4) to mitigate the observation discrepancy between bimanual and unimanual systems for better generalization. Finally, we outline the training objectives (Section 3.5).

3.1. Problem Formulation

The task of policy learning for bimanual manipulation can be defined as follows. To complete a wide range of manipulation tasks specified in natural language, the bimanual agent is required to interactively predict the actions of both end-effectors based on the visual observation and robot states, where the motion is acquired by a low-level planner (*e.g.*, RRT-Connect). The observation o_t at the t_{th} time step includes the voxel v_t converted from RGB and depth images [31, 50] and the robot proprioception p_t . The action a_t for each end-effector at the t_{th} time step contains the location a_{trans} , orientation a_{rot} , gripper open state a_{open} and usage of collision avoidance in the motion planner a_{col} . For the training data, human demonstrators produce a limited set of M offline expert trajectories $\mathcal{D} = \{(o_1, a_1^{left}, a_1^{right}), \dots, (o_M, a_M^{left}, a_M^{right})\}$ for each task instruction l , where a_t^{arm} , $arm \in \mathcal{A} = \{left, right\}$ demonstrates the actions for left and right grippers. Existing methods directly learn the policy model from expert demonstrations, which have shown effectiveness in single-task settings. However, due to the high cost of data collection in bimanual systems, the scarcity of expert demonstrations limits the generalizability of these methods across tasks. To address this, we present to transfer pretrained generalizable

unimanual policy for general bimanual manipulation.

3.2. Overall Pipeline

Overall pipeline of our AnyBimanual method is shown in Figure 2. For the language branch, we employed a pre-trained text encoder [49] to parse the bimanual instruction to language embeddings with high-level semantics, where the skill manager schedules the skill primitives with composition and compensation to enhance the language embeddings that instruct relevant subtasks for different arms. Therefore, the pre-trained unimanual policy model can be prompted to generate feasible manipulation policy for each arm with high generalization ability across tasks with the sharable manipulation knowledge. For the visual branch, we voxelize the RGB-D input to the voxel space as observation, and a 3D sparse voxel encoder is utilized to tokenize the voxel observation for informative volumetric representation. The visual aligner generates a soft spatial mask to align the visual representation of unimanual policy model with its representation during pretraining, so that the observation discrepancy between unimanual and bimanual systems can be minimized for policy transferability enhancement. We employ two pretrained unimanual models to predict the left and right robot actions based on the text embeddings and visual representations, where the pretrained unimanual policy can be multi-modal transformer-based policy [7, 8, 17, 41, 50] or diffusion-based policy [39, 51].

3.3. Scheduling Unimanual Skill Primitives

In order to transfer unimanual manipulation policy to bimanual settings without generalizability drops, we propose a skill manager to decompose the action policies from unimanual foundation models into skill primitives and integrate primitives for bimanual systems. However, the given offline expert demonstrations \mathcal{D} do not contain any explicit intermediate skill primitives or sub-task boundaries, but only low-level end-effector poses and high-level natural language instruction are provided. Therefore, we design an automatic skill discovery method in an unsupervised manner to learn skill representations and their schema from offline bimanual manipulation datasets during training. In the test phase, the skill manager predicts different weighted combinations of primitive skills to orchestrate each arm given high-level language instruction, which enables effective transfer of pre-trained unimanual policy to diverse bimanual manipulation tasks.

Skill Manager. We start with a discrete primitive skill set $\mathcal{Z} = \{z_1, z_2, \dots, z_K\}$, where K is a hyper-parameter that indicates the number of skill primitives. To realize end-to-end skill discovery and scheduling, each potential skill is an implicit embedding $z_k \in \mathbb{R}^D$, which can be initialized with the corresponding language template tokens of the pre-trained unimanual policy to mitigate the domain gap. By

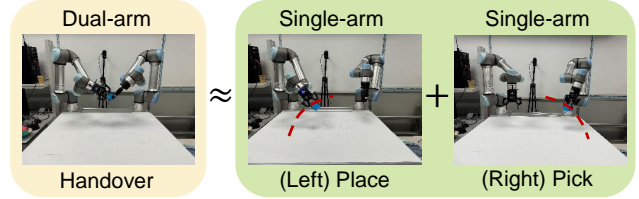


Figure 3. **Shareable skills across unimanual and bimanual settings.** We observe that bimanual tasks are often originated from the combination of unimanual sub-tasks, which thus can be solved by effectively coordinating unimanual skills synchronously or asynchronously.

combining the primitives from the skill set, the language embedding for the unimanual policy model can be represented as a linear combination of these primitives. Hence, the reconstructed language embedding as skill representation can be expressed as:

$$\hat{l}_t^{\text{left}} = \sum_{k=1}^K \hat{w}_{k,t}^{\text{left}} z_k + \epsilon_t^{\text{left}}, \quad \hat{l}_t^{\text{right}} = \sum_{k=1}^K \hat{w}_{k,t}^{\text{right}} z_k + \epsilon_t^{\text{right}} \quad (1)$$

where \hat{l}_t^{arm} is the decomposed unimanual language embedding for one arm of the bimanual system, and $\hat{w}_t^{\text{arm}} \in \mathbb{R}^K$ denotes the importance weight for linear combination for both values of $\text{arm} \in \mathcal{A}$. We also introduce a task-oriented compensation $\epsilon_t^{\text{arm}} \in \mathbb{R}^D$ to introduce the embodiment-specific knowledge for the policy transfer. The upscript arm of the variables can be selected from left or right to indicate the embodiment in the bimanual systems. As depicted in Figure 3, considering a bimanual task `Handover`, it can be explicitly solved by scheduling two unimanual primitive skills, i.e., the left arm `Place` the block to the right gripper while the right arm `Pick` it from the left gripper.

Though every language embedding that passed through the pretrained single policy can be represented as a linear combination of the skill set, the combination weights that specify the importance of each skill are dynamic across the task completion process. We propose to parametrize a multi-model transformer named skill manager to dynamically predict the combination weight for each arm at each time step. Therefore, our skill manager f can be formulated as $(\hat{w}_t^{\text{left}}, \epsilon_t^{\text{left}}, \hat{w}_t^{\text{right}}, \epsilon_t^{\text{right}}) = f_{\theta}(v_t, l, p_t)$, which takes the overall bimanual visual and language embeddings, proprioception as input, and assigns the reconstructed unimanual language embedding for each arm as output to schedule the skill primitive of each arm dynamically. θ represents the learnable parameters. Finally, the combined skill primitives are concatenated with the initial bimanual language embedding to enhance the global context, which is then forwarded to the corresponding unimanual policy.

Learning Generalizable Skill Representations. To update the skill library, we expect the discovered skill representations are informative to encode fundamental robot motions

that are sharable across a variety of tasks, thereby enhancing the generalizability of our framework. To realize this, the learning objective of the skill manager is designed as a sparse representation problem [61]:

$$\mathcal{L}_{\text{skill}} = \|\hat{w}^{\text{left}}\|_1 + \|\hat{w}^{\text{right}}\|_1 + \lambda_\epsilon (\|\epsilon^{\text{left}}\|_{2,1} + \|\epsilon^{\text{right}}\|_{2,1}) \quad (2)$$

where $\|\cdot\|_1$, and $\|\cdot\|_{2,1}$ denote the ℓ_1 and $\ell_{2,1}$ norm, respectively. λ_ϵ is a hyper-parameter that balances the denoising term. By minimizing this sparse regularization term, the skill manager is encouraged to reconstruct the skill representation by selecting fewer skill primitives, which is further surrogated by minimizing a differentiable ℓ_1 regularization [52]. Therefore, the skill subspaces are required to be orthogonal and disjoint with each other to reconstruct the language embedding with sparse combination and compensation, which implicitly enforces each skill representation to capture an independent fundamental motion.

3.4. Aligning Unimanual Visual Representations

Visual Aligner. Despite the skill manager enabling generalization in the language modality, the distributional shift from the unimanual to bimanual workspace in terms of the visual context still may harm the model performance. To mitigate the observation discrepancy, we present a visual aligner q that predict two spatial soft masks at each step t to edit the voxel space so that the decomposed subspace of unimanual policy model for each arm aligns with those during pretraining stage: $(\hat{v}_t^{\text{left}}, \hat{v}_t^{\text{right}}) = q_\theta(v_t, l, p_t)$. The decomposed observation represents the locality of the workspace, which is then augmented by the bimanual observation to form the final visual embedding:

$$v_t^{\text{left}} = (\hat{v}_t^{\text{left}} \odot v_t) \oplus v_t, \quad v_t^{\text{right}} = (\hat{v}_t^{\text{right}} \odot v_t) \oplus v_t, \quad (3)$$

where \odot is the element-wise multiplication, and \oplus refers to the concatenation operator. As a result, the augmented visual representations for each arm contains both embodiment-specific information and the global context, which is then passed through the two unimanual policy models to decode the optimal bimanual action.

Learning Aligned Visual Representations. Our goal is to mitigate the visual domain gap between the unimanual and bimanual setting, so that the pretrained commonsense knowledge in unimanual policy can be transferred with high adaptation ability. Since we can not access the unimanual pretraining data in common usages, we instead impose a mutually exclusive prior to the visual aligner. This prior is regularized by optimizing a Jensen-Shannon (JS) divergence regularization term:

$$\mathcal{L}_{\text{voxel}} = -D_{KL}(\hat{v}_t^{\text{left}} \parallel \hat{v}_t^{\text{right}}) / 2 - D_{KL}(\hat{v}_t^{\text{right}} \parallel \hat{v}_t^{\text{left}}) / 2 \quad (4)$$

where D_{KL} means the Kullback-Leibler (KL) divergence operator. To provide further explanation, bimanual manipulation tasks often involve asynchronous collaboration that

requires the left and right arm to attend to different areas of the whole workspace to act as different roles, such as stabilizing and acting. As a result, the mutually exclusive division of the entire bimanual workspace will naturally separate one arm and its target from the other, which highly resembles the unimanual configuration. Hence by maximizing the divergence between the two soft masks, the voxel input of the bimanual manipulation agent can be disentangled into unimanual visual representations that align with those in the pretraining phase effectively.

3.5. Learning Objectives

The decomposed skill and volumetric representation are used to pass through the two pretrained unimanual policies to predict the optimal actions of the two end-effectors. We assume access to a pretrained unimanual policy p , which is fundamentally a multi-model multi-task neural network that takes visual and language embedding as inputs and outputs end-effector actions. Our AnyBimanual is a model-agnostic plug-and-play method, which indicates that the architecture of pretrained unimanual policy p is flexible in different architectures such as multi-modal transformer-based policies [41, 50] and diffusion policies [39, 51]. To supervise the model with the provided expert demonstrations for behavior cloning, we leverage the cross-entropy loss to learn accurate action prediction for each arm:

$$\mathcal{L}_{\text{BC}} = \sum_{\text{arm} \in \mathcal{A}} CE(p_{\text{trans}}^{\text{arm}}, p_{\text{rot}}^{\text{arm}}, p_{\text{open}}^{\text{arm}}, p_{\text{col}}^{\text{arm}}) \quad (5)$$

where $p_{\text{trans}}^{\text{arm}}, p_{\text{rot}}^{\text{arm}}, p_{\text{open}}^{\text{arm}}, p_{\text{col}}^{\text{arm}}$ represents the distribution of the ground-truth actions for translation, rotation, gripper openness, and collision avoidance for the corresponding robot arm, respectively. The behavior cloning loss is then combined with the two regularization terms described above to learn informative skill manager and visual aligner. To sum up, the training objective of AnyBimanual is:

$$\mathcal{L}_{\text{total}} = \mathcal{L}_{\text{BC}} + \lambda_{\text{skill}} \mathcal{L}_{\text{skill}} + \lambda_{\text{voxel}} \mathcal{L}_{\text{voxel}}, \quad (6)$$

where λ_{skill} and λ_{voxel} refer to hyper-parameters that balance the importance of the regularizations.

4. Experiments

In this section, we first introduce the experimental setups (Section 4.1). Then, we transfer various unimanual methods to bimanual manipulation via AnyBimanual, and compare them with the state-of-the-art to show superiority (Section 4.2). We conduct an ablation study to evaluate validity of the proposed components (Section 4.3). We further interpret learned skill representation and decomposed volumetric representation by visualization (Section 4.4). Finally, we report real-robot results to demonstrate effectiveness of AnyBimanual in real-world applications (Section 4.5).

Table 1. **Multi-Task Test Results in Simulator.** Average success rates (%) of general bimanual manipulation agents trained with 20 or 100 demonstrations per task and evaluated over 100 episodes. ‘LF’ means the leader-follower architecture that transfers unimanual manipulation policy for bimanual manipulation. AnyBimanual enables plug-and-play transfers for multiple unimanual manipulation policies.

Method	pick laptop		pick plate		straighten rope		lift ball		lift tray		push box	
	20	100	20	100	20	100	20	100	20	100	20	100
RVT [28]-LF	1	2	1	1	1	2	3	3	4	6	7	18
RVT-LF + AnyBimanual	1	3	2	4	2	5	3	4	4	6	11	21
PerAct [50]-LF	1	2	3	4	5	11	4	7	6	12	7	17
PerAct-LF + AnyBimanual	2	2	3	5	12	14	8	8	15	17	23	29
PerAct ² [31]	3	4	2	4	6	8	4	4	4	3	5	6
PerAct ² + Pretraining	3	5	5	7	13	17	9	14	2	5	23	31
PerAct + AnyBimanual	4	7	6	8	17	24	22	36	9	14	31	46

Method	put in fridge		press buttons		handover item		sweep to dustpan		take out tray		handover easy	
	20	100	20	100	20	100	20	100	20	100	20	100
RVT [28]-LF	0	0	10	22	0	0	0	0	2	2	3	3
RVT-LF + AnyBimanual	1	3	17	32	1	2	4	13	1	2	2	7
PerAct [50]-LF	2	7	2	9	0	3	22	47	0	3	2	5
PerAct-LF + AnyBimanual	4	9	12	14	1	5	34	57	1	4	3	13
PerAct ² [31]	7	16	23	41	3	6	25	52	1	3	22	29
PerAct ² + Pretraining	10	22	27	40	3	7	29	55	3	8	24	33
PerAct + AnyBimanual	13	26	39	73	7	15	43	67	9	24	31	44

Table 2. **Comparison of AnyBimanual with Different Techniques.** We categorize the long-term tasks that require more than 6.5 keyframes to Long, tasks that involve multiple variations to Generalized and tasks that involve synchronization of both arms to Sync for further interpretability.

Row ID	Skill Manager	Visual Aligner	Long	Generalized	Sync	Average
1	-	-	16.29	23.50	3.50	14.67
2	✗	✗	19.57	25.50	9.50	16.75
3	✗	✓	21.57	44.00	15.50	19.75
4	✓	✗	23.71	42.00	17.00	25.67
5	✓	✓	27.29	44.00	25.00	32.00

4.1. Experiment Setup

Simulation. For benchmarking, our simulation experiments are conducted on RLBench2 [31], a bimanual version extended from the widely-used RLBench [36] benchmark in prior works [28, 35, 39, 47, 63, 69]. Following the setup in [31], we utilize 12 language-conditioned bimanual manipulation tasks varying from different challenge levels. The diverse task suite requires the agent to acquire and correctly schedule shareable skills to achieve high success rates, rather than merely imitating limited expert demonstrations. For observation, we employ six cameras with a resolution of 256×256 to cover the entire workspace. During the training phase, we provide 20 or 100 demonstrations for each task, and we evaluate 100 episodes per task in the testing set to mitigate the randomness.

Real Robot. The real-world setup for our experiments involves two Universal Robots UR5e manipulators equipped with Robotiq 2F-85 grippers, controlled by two Xbox joysticks for collecting demonstrations. A calibrated front RGB-D Realsense camera provides 640×480 resolution

images at 30 Hz for observation. We collect 30 real-world human demonstrations per task for training, while the evaluations are conducted using a Nvidia RTX 4080 GPU.

Baselines. We compare our AnyBimanual with the state-of-the-art general bimanual manipulation agents, including the voxel-based method PerAct² [31] and its leader-follower version PerAct-LF, both are modified from the well-known unimanual policy PerAct [50], as well as the multi-view image-based method RVT [28]-LF. To exclude the influence of model parameters, we also implement a counterpart that directly combines two pre-trained PerAct [50] policies. Note that the proposed method is model-agnostic, which supports different communication mechanisms between single-arm policies, and thus we transfer all 3 baselines to validate the versatility of AnyBimanual. The evaluation metric is the task success rate, which is defined as the percentage of episodes where the agent successfully completes the instructed goal within 25 steps.

Implementation Details. Following the common training recipe [28, 31, 50], we use the SE(3) observation augmentation for the expert demonstrations in the training set to improve the robustness of the agents. For fair comparisons, all compared methods are trained for 100k iterations on two NVIDIA RTX 3090 GPUs with a total batch size of 4. We use the LAMB optimizer [67] with a constant learning rate of 5×10^{-4} to update model parameters, in line with the previous arts [28, 31, 50].

4.2. Comparison with the State-of-the-Art Methods

In this section, we compare our AnyBimanual with previous state-of-the-art approaches on RLBench tasksuite. Ta-

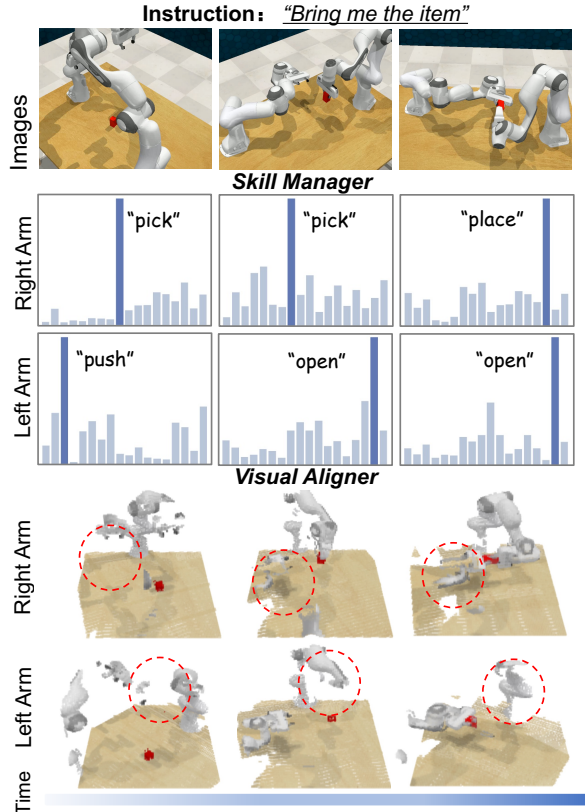


Figure 4. **Visualization of AnyBimanual.** This figure shows in different key timesteps, how the skill manager dynamically schedules skill weights and how the visual aligner decomposes volumetric observation. We use a logarithmic scale for visualization.

ble 1 presents a comparison of the average success rates for each task and the average performance is shown in Figure 1. Our method achieves the highest overall performance, with an average success rate of 32.00%, setting a new state-of-the-art in general bimanual manipulation. AnyBimanual leverages the knowledge distilled from unimanual models and successfully transfers it to guide general bimanual manipulation. As a result, our method outperforms the cutting-edge bimanual method PerAct² by a significant improvement of 17.33% on average. With a limited set of 20 demonstrations, our method still defeats the baseline with a sizable margin of 10.50%. Note that we aim to train multi-task agents to handle a wide range of tasks within a single model, hence the performance is lower than the reported in the original paper. Especially, we observe that AnyBimanual shows greater improvement in long-horizon tasks like `put in fridge`, multi-variations tasks like `press buttons`, and tasks demand synchronous coordinations like `straighten rope`. Moreover, AnyBimanual enables plug-and-play transferring of PerAct-LF and RVT, which also leads to relative boosts of 72.76% (4.92% to 8.50%) and 39.41% (10.58% to 14.75%) on average. However, incorporating

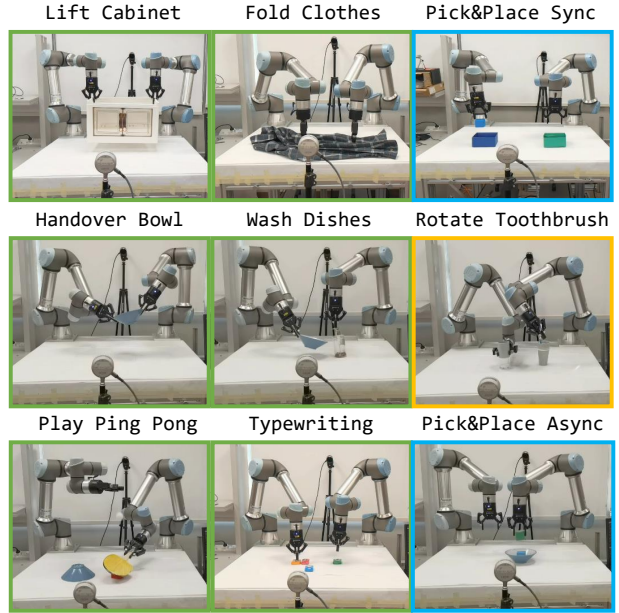


Figure 5. **Real-World Tasks.** The real-world experiments are performed in a tabletop setup with objects randomized in location every episode. AnyBimanual can simultaneously conduct 9 complex real-world bimanual manipulation tasks with one model. Different colors mean different success rates.

AnyBimanual slightly affects the performance on the simple, short-horizon `Lift ball`, due to the additional complexity in input processing.

4.3. Ablation Study

Our AnyBimanual framework leverages a skill manager to dynamically coordinate unimanual skills, while mitigating the distributional shift between unimanual and bimanual visual inputs with a visual aligner. We conduct an ablation study in Table 2 by transferring the powerful unimanual baseline PerAct [50] to bimanual tasks. We first implement a vanilla baseline without any of the proposed techniques (Row 1), where we load the pre-trained PerAct model and directly finetune the baseline to predict bimanual action, which shows enhanced long-horizon task execution and generalizability with an unneglected performance drop in tasks that require proper coordination.

Skill Manager. By employing the skill manager in the experiment, we observe that the average success rate increases by 8.92% (Row 4 vs. Row 2). Notably, in tasks requiring long-term manipulation within the `Long` category, it significantly outperforms the vanilla version, demonstrating the skill manager’s effectiveness in long-horizon tasks.

Visual Aligner. Additionally, we incorporate the spatial soft masking from the visual aligner, resulting in a substantial performance improvement of 3.00% (Row 3 vs. Row 2). Although the inclusion of spatial soft masking mechanism may slightly affect performance in simpler tasks due to in-

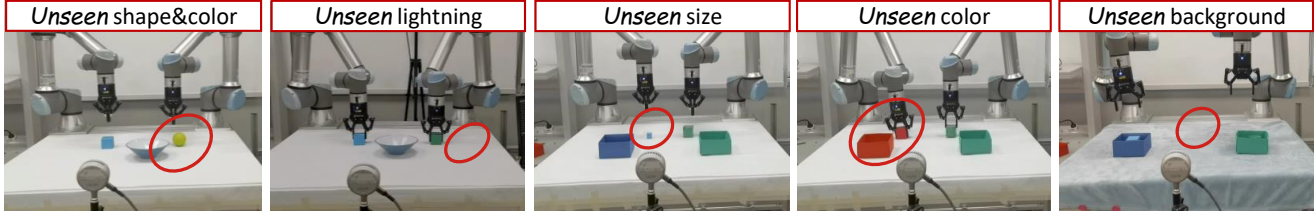


Figure 6. **Unseen Data Generalization.** We include multiple distractors in real-world experiments, and find AnyBimanual generalizes to these settings successfully by unlocking the commonsense held by unimanual base models.

creased input processing complexity, it leads to significant gains in overall task success. The gains are even more notable in *Generalized* and *Sync* tasks, which demand a high degree of adaptability to scene variations and synchronization for cooperative actions. The results demonstrate the visual aligner preserves the generalizability stored in the unimanual policy perfectly, facilitating seamless coordination between the arms. By integrating all techniques in our AnyBimanual, the success rate improves from 14.67% to 32.00% (Row 5), validating the importance of properly mining unimanual knowledge for bimanual manipulation.

4.4. Qualitative Analysis

In Figure 4, we visualize linear combination of the skill set and the decomposition of volumetric observation in one complete task to further interpret AnyBimanual. For illustration, we use 18 task embeddings from PerAct [50] as the initial skill set and explicit soft mask. At timestep 1, the right arm primarily follows the `pick blocks` in `sorter` task (*skill* 7) from the skill set, as the right arm needs to pick up a block from the table at first. The left arm is guided by the `push button` task (*skill* 2), as its motion only involves a downward push without interacting with any objects. At timestep 2, the right arm holds the red block stationary, and the left arm approaches and grasps it, similar to the motion in `open drawer` task (*skill* 16). Additionally, the visual aligner effectively decomposes the voxel space, allowing each arm to focus on relevant information. For instance, at timestep 2, details of the right arm are soft-masked in the left arm’s voxel (as shown in the circled area), which allows the left arm only focus on the red cube without interference from the other arm, enabling the left arm to grasp the red cube more effectively.

4.5. Real-Robot Results

We further validate our approach through real-robot experiments. We train one multi-task AnyBimanual agent that transfers the unimanual policy PerAct [50] to 9 real-world tasks and report the average success rates on Table 3. Guided by [42], these tasks are designed to cover different challenge levels, such as synchronous and asynchronous coordination, short and long-horizon execu-

Table 3. **Real-world Results.** Average success rates (%) of our multi-task model trained and evaluated on 9 real-world tasks.

Task	Sync.	Object	Variation	Episode	Keyframe	Average
Lift Cabinet	✓	1	1	5	3.0	100.0
Fold Clothes	✓	1	1	5	3.0	100.0
Pick&Place Sync	✓	7	3	15	3.0	80.0
Handover Bowl	✗	1	1	5	4.0	100.0
Wash Dishes	✗	2	1	5	4.0	100.0
Play Ping Pong	✗	3	1	5	3.0	100.0
Rotate Toothbrush	✗	3	1	5	4.0	20.0
Typewriting	✗	4	1	5	6.0	100.0
Pick&Place Async	✗	5	3	15	4.0	80.0

tion, etc. In the real-robot experiments, our keyframes are manually extracted, providing more stable task guidance compared to heuristic extraction methods in simulation. The overall success rate across 65 test episodes in total is 84.62%, which illustrates a significant practicality of AnyBimanual in real-world settings. Especially, in multi-variant tasks that require high generalizability like `Pick&Place Sync` and `Pick&Place Async` shown in Figure 6, our AnyBimanual completes 80% tasks of different initial positions, object colors, object size, lighting and backgrounds successfully. The failure cases occur on tasks that demand precise rotation, e.g., `Rotate Toothbrush`, which could be mitigated by leveraging high-capacity unimanual policy [41] or balancing the weight of the rotation term in behavior cloning.

5. Conclusion

In this paper, we have introduced AnyBimanual, a framework designed to transfer pretrained unimanual manipulation policies to multi-task bimanual manipulation with few bimanual demonstrations. We develop a skill manager to dynamically schedule skill primitives discovered from unimanual policies, enabling their effective adaptation for bimanual tasks. To address the observation discrepancies between unimanual and bimanual systems, we propose a visual aligner that generates spatial soft masks, aligning the visual embeddings of each arm with those used during the pretraining stage of the unimanual policy model. Extensive experiments across 12 simulated and 9 real-world tasks demonstrate the effectiveness of AnyBimanual. The limitations are discussed in the supplementary file.

References

- [1] Michael Ahn, Debidatta Dwibedi, Chelsea Finn, Montse Gonzalez Arenas, Keerthana Gopalakrishnan, Karol Hausman, Brian Ichter, Alex Irpan, Nikhil Joshi, Ryan Julian, et al. Autort: Embodied foundation models for large scale orchestration of robotic agents. *arXiv preprint arXiv:2401.12963*, 2024. 2
- [2] Fabio Amadio, Adrià Colomé, and Carme Torras. Exploiting symmetries in reinforcement learning of bimanual robotic tasks. *IEEE Robotics and Automation Letters (RAL)*, 4(2): 1838–1845, 2019. 3
- [3] Yahav Avigal, Lars Berscheid, Tamim Asfour, Torsten Kröger, and Ken Goldberg. Speedfolding: Learning efficient bimanual folding of garments. In *Proceedings of the IEEE/RSJ International Conference on Intelligent Robots and Systems (IROS)*, pages 1–8. IEEE, 2022.
- [4] Aleksandar Batinica, Bojan Nemeč, Aleš Ude, Mirko Raković, and Andrej Gams. Compliant movement primitives in a bimanual setting. In *IEEE-RAS International Conference on Humanoid Robotics (Humanoids)*, pages 365–371, 2017. 3
- [5] Peter Baumgartner, Alexander Fuchs, and Cesare Tinelli. Lemma learning in the model evolution calculus. In *International Conference on Logic for Programming Artificial Intelligence and Reasoning (LPAR)*, pages 572–586, 2006. 2
- [6] Christian Bersch, Benjamin Pitzer, and Sören Kammel. Bimanual robotic cloth manipulation for laundry folding. In *Proceedings of Robotics: Science and Systems (RSS)*, pages 1413–1419, 2011. 2
- [7] Anthony Brohan, Noah Brown, Justice Carbajal, Yevgen Chebotar, Joseph Dabis, Chelsea Finn, Keerthana Gopalakrishnan, Karol Hausman, Alex Herzog, Jasmine Hsu, et al. Rt-1: Robotics transformer for real-world control at scale. In *Proceedings of Robotics: Science and Systems (RSS)*, 2023. 2, 4
- [8] Anthony Brohan, Noah Brown, Justice Carbajal, Yevgen Chebotar, et al. Rt-2: Vision-language-action models transfer web knowledge to robotic control. In *Conference on Robot Learning (CoRL)*, pages 2165–2183, 2023. 2, 4
- [9] Jens F Buhl, Rune Grønhøj, Jan K Jørgensen, Guilherme Mateus, Daniela Pinto, Jacob K Sørensen, Simon Bøgh, and Dimitrios Chrysostomou. A dual-arm collaborative robot system for the smart factories of the future. *Procedia manufacturing*, 38:333–340, 2019. 1, 2
- [10] Xi Chen, Xiao Wang, Lucas Beyer, Alexander Kolesnikov, Jialin Wu, Paul Voigtlaender, Basil Mustafa, Sebastian Goodman, Ibrahim Alabdulmohsin, Piotr Padlewski, et al. Pali-3 vision language models: Smaller, faster, stronger. *arXiv preprint arXiv:2310.09199*, 2023. 2
- [11] Yuanpei Chen, Yiran Geng, Fangwei Zhong, Jiaming Ji, Jiechuang Jiang, Zongqing Lu, Hao Dong, and Yaodong Yang. Bi-dexhands: Towards human-level bimanual dexterous manipulation. *IEEE Transactions on Pattern Analysis and Machine Intelligence (T-PAMI)*, 46(5):2804–2818, 2024. 2
- [12] Xuxin Cheng, Jialong Li, Shiqi Yang, Ge Yang, and Xiaolong Wang. Open-television: Teleoperation with immersive active visual feedback. *arXiv preprint arXiv:2407.01512*, 2024. 2
- [13] Cheng Chi, Zhenjia Xu, Chuer Pan, Eric Cousineau, Benjamin Burchfiel, Siyuan Feng, Russ Tedrake, and Shuran Song. Universal manipulation interface: In-the-wild robot teaching without in-the-wild robots. *arXiv preprint arXiv:2402.10329*, 2024. 2
- [14] Rohan Chitnis, Shubham Tulsiani, Saurabh Gupta, and Abhinav Gupta. Intrinsic motivation for encouraging synergistic behavior. In *Proceedings of the International Conference on Learning Representations (ICLR)*, 2020. 3
- [15] Rohan Chitnis, Shubham Tulsiani, Saurabh Gupta, and Abhinav Gupta. Efficient bimanual manipulation using learned task schemas. In *IEEE International Conference on Robotics and Automation (ICRA)*, pages 1149–1155, 2020. 2, 3
- [16] Ian Chuang, Andrew Lee, Dechen Gao, and Iman Soltani. Active vision might be all you need: Exploring active vision in bimanual robotic manipulation. *arXiv preprint arXiv:2409.17435*, 2024. 2
- [17] Embodiment Collaboration and Abby O’Neill et al. Open x-embodiment: Robotic learning datasets and rt-x models. In *Proceedings of the IEEE International Conference on Robotics and Automation (ICRA)*, pages 6892–6903, 2024. 2, 4
- [18] Runyu Ding, Yuzhe Qin, Jiyue Zhu, Chengzhe Jia, Shiqi Yang, Ruihan Yang, Xiaojuan Qi, and Xiaolong Wang. Bunny-visionpro: Real-time bimanual dexterous teleoperation for imitation learning. *arXiv preprint arXiv:2407.03162*, 2024. 2
- [19] Giovanni Franzese, Leandro de Souza Rosa, Tim Verburg, Luka Peternel, and Jens Kober. Interactive imitation learning of bimanual movement primitives. *IEEE/ASME Transactions on Mechatronics (T-Mech)*, 2023. 3
- [20] Daocheng Fu, Xin Li, Licheng Wen, Min Dou, Pinlong Cai, Botian Shi, and Yu Qiao. Drive like a human: Rethinking autonomous driving with large language models. In *IEEE/CVF Winter Conference on Applications of Computer Vision (WACV)*, pages 910–919, 2024. 3
- [21] Letian Fu, Huang Huang, Lars Berscheid, Hui Li, Ken Goldberg, and Sachin Chitta. Safe self-supervised learning in real of visuo-tactile feedback policies for industrial insertion. In *Proceedings of the IEEE International Conference on Robotics and Automation (ICRA)*, pages 10380–10386, 2023. 3
- [22] Zipeng Fu, Tony Z Zhao, and Chelsea Finn. Mobile aloha: Learning bimanual mobile manipulation with low-cost whole-body teleoperation. *arXiv preprint arXiv:2401.02117*, 2024. 2
- [23] Aditya Ganapathi, Priya Sundaesan, Brijen Thananjeyan, Ashwin Balakrishna, Daniel Seita, Jennifer Grannen, Minh Hwang, Ryan Hoque, Joseph E Gonzalez, Nawid Jamali, et al. Learning dense visual correspondences in simulation to smooth and fold real fabrics. In *Proceedings of the IEEE International Conference on Robotics and Automation (ICRA)*, pages 11515–11522, 2021. 3
- [24] Jianfeng Gao, Xiaoshu Jin, Franziska Krebs, Noémie Jaquier, and Tamim Asfour. Bi-kvil: Keypoints-based visual

- imitation learning of bimanual manipulation tasks. In *Proceedings of the IEEE International Conference on Robotics and Automation (ICRA)*, pages 16850–16857, 2024. 2
- [25] Zeyu Gao, Yao Mu, Jinye Qu, Mengkang Hu, Lingyue Guo, Ping Luo, and Yanfeng Lu. Dag-plan: Generating directed acyclic dependency graphs for dual-arm cooperative planning. *arXiv preprint arXiv:2406.09953*, 2024. 7
- [26] Zeyu Gao, Yao Mu, Jinye Qu, Mengkang Hu, Lingyue Guo, Ping Luo, and Yanfeng Lu. Dag-plan: Generating directed acyclic dependency graphs for dual-arm cooperative planning. *arXiv preprint arXiv:2406.09953*, 2024. 2
- [27] Koffivi Fidèle Gbagbe, Miguel Altamirano Cabrera, Ali Alabbas, Oussama Alyunes, Artem Lykov, and Dzmityr Tsetserukou. Bi-vla: Vision-language-action model-based system for bimanual robotic dexterous manipulations. *arXiv preprint arXiv:2405.06039*, 2024. 2
- [28] Ankit Goyal, Jie Xu, Yijie Guo, Valts Blukis, Yu-Wei Chao, and Dieter Fox. Rvt: Robotic view transformer for 3d object manipulation. In *Conference on Robot Learning (CoRL)*, pages 694–710, 2023. 6
- [29] Jennifer Grannen, Priya Sundaresan, Brijen Thananjeyan, Jeffrey Ichnowski, Ashwin Balakrishna, Vainavi Viswanath, Michael Laskey, Joseph Gonzalez, and Ken Goldberg. Untangling dense knots by learning task-relevant keypoints. In *Conference on Robot Learning (CoRL)*, pages 782–800, 2020. 3
- [30] Jennifer Grannen, Yilin Wu, Brandon Vu, and Dorsa Sadigh. Stabilize to act: Learning to coordinate for bimanual manipulation. In *Conference on Robot Learning (CoRL)*, pages 563–576, 2023. 1, 2
- [31] Markus Grotz, Mohit Shridhar, Yu-Wei Chao, Tamim Asfour, and Dieter Fox. Peract2: Benchmarking and learning for robotic bimanual manipulation tasks. In *Conference on Robot Learning (CoRL)*, 2024. 1, 2, 3, 6
- [32] Huy Ha and Shuran Song. Flingbot: The unreasonable effectiveness of dynamic manipulation for cloth unfolding. In *Conference on Robot Learning (CoRL)*, pages 24–33, 2021. 3
- [33] Zhaoyang Jacopo Hu, Ziwei Wang, Yanpei Huang, Aran Sena, Ferdinando Rodriguez y Baena, and Etienne Burdet. Towards human-robot collaborative surgery: Trajectory and strategy learning in bimanual peg transfer. *IEEE Robotics and Automation Letters (RAL)*, 8(8):4553–4560, 2023. 1, 2
- [34] Wenlong Huang, Chen Wang, Ruohan Zhang, Yunzhu Li, Jiajun Wu, and Li Fei-Fei. Voxposer: Composable 3d value maps for robotic manipulation with language models. In *Conference on Robot Learning (CoRL)*, pages 540–562, 2023. 2
- [35] Andrew Jaegle, Felix Gimeno, Andy Brock, Oriol Vinyals, Andrew Zisserman, and Joao Carreira. Perceiver: General perception with iterative attention. In *Proceedings of the International Conference on Machine Learning (ICML)*, pages 4651–4664, 2021. 6
- [36] Stephen James, Zicong Ma, David Rovick Arrojo, and Andrew J Davison. Rlbench: The robot learning benchmark & learning environment. *IEEE Robotics and Automation Letters (RAL)*, 5(2):3019–3026, 2020. 6, 1
- [37] Frank Joublin, Antonello Ceravola, Pavel Smirnov, Felix Ocker, Joerg Deigmoeller, Anna Belardinelli, Chao Wang, Stephan Hasler, Daniel Tanneberg, and Michael Gienger. Copal: corrective planning of robot actions with large language models. In *Proceedings of the IEEE International Conference on Robotics and Automation (ICRA)*, pages 8664–8670, 2024. 2
- [38] Satoshi Kataoka, Seyed Kamyar Seyed Ghasemipour, Daniel Freeman, and Igor Mordatch. Bi-manual manipulation and attachment via sim-to-real reinforcement learning. *arXiv preprint arXiv:2203.08277*, 2022. 2
- [39] Tsung-Wei Ke, Nikolaos Gkanatsios, and Katerina Fragkiadaki. 3d diffuser actor: Policy diffusion with 3d scene representations. *arXiv preprint arXiv:2402.10885*, 2024. 2, 4, 5, 6
- [40] Alexander Khazatsky, Karl Pertsch, Suraj Nair, Ashwin Balakrishna, Sudeep Dasari, Siddharth Karamcheti, Soroush Nasiriany, Mohan Kumar Srirama, Lawrence Yunliang Chen, Kirsty Ellis, et al. Droid: A large-scale in-the-wild robot manipulation dataset. *arXiv preprint arXiv:2403.12945*, 2024. 2
- [41] Moo Jin Kim, Karl Pertsch, Siddharth Karamcheti, Ted Xiao, Ashwin Balakrishna, Suraj Nair, Rafael Rafailov, Ethan Foster, Grace Lam, Pannag Sanketi, et al. Openvla: An open-source vision-language-action model. *arXiv preprint arXiv:2406.09246*, 2024. 2, 4, 5, 8
- [42] Franziska Krebs and Tamim Asfour. A bimanual manipulation taxonomy. *IEEE Robotics and Automation Letters (RAL)*, 7(4):11031–11038, 2022. 8, 1, 3
- [43] Zhixuan Liang, Yao Mu, Hengbo Ma, Masayoshi Tomizuka, Mingyu Ding, and Ping Luo. Skilldiffuser: Interpretable hierarchical planning via skill abstractions in diffusion-based task execution. In *Proceedings of the IEEE Conference on Computer Vision and Pattern Recognition (CVPR)*, pages 16467–16476, 2024. 3
- [44] Bo Liu, Yuqian Jiang, Xiaohan Zhang, Qiang Liu, Shiqi Zhang, Joydeep Biswas, and Peter Stone. Llm+ p: Empowering large language models with optimal planning proficiency. *arXiv preprint arXiv:2304.11477*, 2023. 2
- [45] I Liu, Chun Arthur, Sicheng He, Daniel Seita, and Gaurav Sukhatme. Voxact-b: Voxel-based acting and stabilizing policy for bimanual manipulation. *arXiv preprint arXiv:2407.04152*, 2024. 1, 2
- [46] Songming Liu, Lingxuan Wu, Bangguo Li, Hengkai Tan, Huayu Chen, Zhengyi Wang, Ke Xu, Hang Su, and Jun Zhu. Rdt-1b: a diffusion foundation model for bimanual manipulation. *arXiv preprint arXiv:2410.07864*, 2024. 2
- [47] Guanxing Lu, Shiyi Zhang, Ziwei Wang, Changliu Liu, Jiwen Lu, and Yansong Tang. Manigaussian: Dynamic gaussian splatting for multi-task robotic manipulation. In *European Conference on Computer Vision (ECCV)*, pages 349–366, 2025. 6
- [48] Asim Munawar, Giovanni De Magistris, Tu-Hoa Pham, Daiki Kimura, Michiaki Tatsubori, Takao Moriyama, Ryuki Tachibana, and Grady Booch. Maestrob: A robotics framework for integrated orchestration of low-level control and high-level reasoning. In *Proceedings of the IEEE Inter-*

- national Conference on Robotics and Automation (ICRA)*, pages 527–534, 2018. 3
- [49] Alec Radford, Jong Wook Kim, Chris Hallacy, Aditya Ramesh, Gabriel Goh, Sandhini Agarwal, Girish Sastry, Amanda Askell, Pamela Mishkin, Jack Clark, et al. Learning transferable visual models from natural language supervision. In *Proceedings of the International Conference on Machine Learning (ICML)*, pages 8748–8763, 2021. 4
- [50] Mohit Shridhar, Lucas Manuelli, and Dieter Fox. Perceiver-actor: A multi-task transformer for robotic manipulation. In *Conference on Robot Learning (CoRL)*, pages 785–799, 2023. 2, 3, 4, 5, 6, 7, 8
- [51] Octo Model Team, Dibya Ghosh, Homer Walke, Karl Pertsch, Kevin Black, Oier Mees, Sudeep Dasari, Joey Hejna, Tobias Kreiman, Charles Xu, et al. Octo: An open-source generalist robot policy. *arXiv preprint arXiv:2405.12213*, 2024. 2, 4, 5
- [52] Robert Tibshirani. Regression shrinkage and selection via the lasso. *Journal of the Royal Statistical Society Series B: Statistical Methodology*, 58(1):267–288, 1996. 5
- [53] Hugo Touvron, Louis Martin, Kevin Stone, Peter Albert, Amjad Almahairi, Yasmine Babaei, Nikolay Bashlykov, Soumya Batra, Prajjwal Bhargava, Shruti Bhosale, et al. Llama 2: Open foundation and fine-tuned chat models. *arXiv preprint arXiv:2307.09288*, 2023. 2
- [54] Jake Varley, Sumeet Singh, Deepali Jain, Krzysztof Choromanski, Andy Zeng, Somnath Basu Roy Chowdhury, Avinava Dubey, and Vikas Sindhwani. Embodied ai with two arms: Zero-shot learning, safety and modularity. *arXiv preprint arXiv:2404.03570*, 2024. 2
- [55] Homer Rich Walke, Kevin Black, Tony Z Zhao, Quan Vuong, Chongyi Zheng, Philippe Hansen-Estruch, Andre Wang He, Vivek Myers, Moo Jin Kim, Max Du, et al. Bridgedata v2: A dataset for robot learning at scale. In *Conference on Robot Learning (CoRL)*, pages 1723–1736, 2023. 2
- [56] Chen Wang, Haochen Shi, Weizhuo Wang, Ruohan Zhang, Li Fei-Fei, and C Karen Liu. Dexcap: Scalable and portable mocap data collection system for dexterous manipulation. *arXiv preprint arXiv:2403.07788*, 2024. 2
- [57] Guanzhi Wang, Yuqi Xie, Yunfan Jiang, Ajay Mandlekar, Chaowei Xiao, Yuke Zhu, Linxi Fan, and Anima Anandkumar. Voyager: An open-ended embodied agent with large language models. *Transactions on Machine Learning Research (TMLR)*, 2024, 2024. 3
- [58] Lirui Wang, Xinlei Chen, Jialiang Zhao, and Kaiming He. Scaling proprioceptive-visual learning with heterogeneous pre-trained transformers. *arXiv preprint arXiv:2409.20537*, 2024. 6
- [59] Su Wang, Chitwan Saharia, Ceslee Montgomery, Jordi Pont-Tuset, Shai Noy, Stefano Pellegrini, Yasumasa Onoe, Sarah Laszlo, David J Fleet, Radu Soricut, et al. Imagen editor and editbench: Advancing and evaluating text-guided image inpainting. In *Proceedings of the IEEE Conference on Computer Vision and Pattern Recognition (CVPR)*, pages 18359–18369, 2023. 6
- [60] Woodrow Zhouyuan Wang, Andy Shih, Annie Xie, and Dorsa Sadigh. Influencing towards stable multi-agent inter- actions. In *Conference on Robot Learning (CoRL)*, pages 1132–1143, 2022. 2
- [61] John Wright, Yi Ma, Julien Mairal, Guillermo Sapiro, Thomas S Huang, and Shuicheng Yan. Sparse representation for computer vision and pattern recognition. *Proceedings of the IEEE*, 98(6):1031–1044, 2010. 5
- [62] Philipp Wu, Yide Shentu, Zhongke Yi, Xingyu Lin, and Pieter Abbeel. Gello: A general, low-cost, and intuitive teleoperation framework for robot manipulators. *arXiv preprint arXiv:2309.13037*, 2023. 2
- [63] Zhou Xian, Nikolaos Gkanatsios, Theophile Gervet, Tsung-Wei Ke, and Katerina Fragkiadaki. Chaineddiffuser: Unifying trajectory diffusion and keypose prediction for robotic manipulation. In *Conference on Robot Learning (CoRL)*, pages 2323–2339, 2023. 6
- [64] Fan Xie, Alexander Chowdhury, M. Clara De Paolis Kaluza, Linfeng Zhao, Lawson L. S. Wong, and Rose Yu. Deep imitation learning for bimanual robotic manipulation. In *Advances in Neural Information Processing Systems (NeurIPS)*, 2020. 3
- [65] Shiqi Yang, Minghuan Liu, Yuzhe Qin, Runyu Ding, Jialong Li, Xuxin Cheng, Ruihan Yang, Sha Yi, and Xiaolong Wang. Ace: A cross-platform visual-exoskeletons system for low-cost dexterous teleoperation. *arXiv preprint arXiv:2408.11805*, 2024. 2
- [66] Xiaochuan Yin and Qijun Chen. Learning nonlinear dynamical system for movement primitives. In *IEEE International Conference on Systems, Man, and Cybernetics (SMC)*, pages 3761–3766, 2014. 3
- [67] Yang You, Jing Li, Sashank J. Reddi, Jonathan Hseu, Sanjiv Kumar, Srinadh Bhojanapalli, Xiaodan Song, James Demmel, Kurt Keutzer, and Cho-Jui Hsieh. Large batch optimization for deep learning: Training BERT in 76 minutes. In *Proceedings of the International Conference on Learning Representations (ICLR)*, 2020. 6, 3
- [68] Dongjie Yu, Hang Xu, Yizhou Chen, Yi Ren, and Jia Pan. Birk: Keypose-conditioned consistency policy for bimanual robotic manipulation. *arXiv preprint arXiv:2406.10093*, 2024. 2
- [69] Yanjie Ze, Ge Yan, Yueh-Hua Wu, Annabella Macaluso, Yuying Ge, Jianglong Ye, Nicklas Hansen, Li Erran Li, and Xiaolong Wang. Gnfactor: Multi-task real robot learning with generalizable neural feature fields. In *Conference on Robot Learning (CoRL)*, pages 284–301, 2023. 6
- [70] Jesse Zhang, Jiahui Zhang, Karl Pertsch, Ziyi Liu, Xiang Ren, Minsuk Chang, Shao-Hua Sun, and Joseph J. Lim. Bootstrap your own skills: Learning to solve new tasks with large language model guidance. In *Conference on Robot Learning (CoRL)*, pages 302–325. PMLR, 2023. 2
- [71] Minghao Zhang, Pingcheng Jian, Yi Wu, Huazhe Xu, and Xiaolong Wang. Dair: Disentangled attention intrinsic regularization for safe and efficient bimanual manipulation. *arXiv preprint arXiv:2106.05907*, 2021. 2
- [72] Tianle Zhang, Dongjiang Li, Yihang Li, Zecui Zeng, Lin Zhao, Lei Sun, Yue Chen, Xuelong Wei, Yibing Zhan, Lusong Li, et al. Empowering embodied manipulation: A bimanual-mobile robot manipulation dataset for household tasks. *arXiv preprint arXiv:2405.18860*, 2024. 1, 2

- [73] Tony Z. Zhao, Vikash Kumar, Sergey Levine, and Chelsea Finn. Learning fine-grained bimanual manipulation with low-cost hardware. In *Proceedings of Robotics: Science and Systems (RSS)*, 2023. [2](#)

AnyBimanual: Transferring Unimanual Policy for General Bimanual Manipulation

Supplementary Material

6. Additional Experimental Details

6.1. Simulation

We utilize RLbench2 [31] as our main simulated task suite for multi-task learning. Table 5 is an overview of the 12 selected tasks we use in the experiments. Table 4 is an overview of the 18 selected tasks from RLbench [36] used to pretrain the unimanual checkpoint. The task variations include randomly sampled colors, sizes, counts, placements, and categories of objects. Other properties vary depending on the specific task. Furthermore, objects are randomly arranged on the tabletop within a certain range, adding to the diversity of the tasks. The visual observation includes 6 RGB-D frames of 256×256 resolutions (*i.e.*, front, shoulder left, shoulder right, wrist left, wrist right and overhead), which are shown in Figure 7. In the ablation study, we group the RLbench2 tasks of Table 5 into 3 categories according to their key challenges. The task groups include:

- The Long group includes long-term tasks that requires more than 6.5 keyframes. The included tasks are: pick plate, pick laptop, put in fridge, handover item, sweep to dustpan, take out of tray and handover easy.
- The Generalized group includes tasks with multiple variations, which are differentiated by instructions. The included tasks are: press buttons and handover item.
- The Sync group requires precise coordination, which often causes failures due to asynchronous manipulation. The included tasks are: lift ball, lift tray, straighten rope and push box.

6.2. Real-Robot

Hardware Setup. The real robot setup uses two Universal Robots UR5e manipulators, each equipped with a Robotiq 2F-85 gripper. See Figure 8 for reference. For the perception, we use a Realsense RGB-D camera mounted on a tripod, positioned to mimic the viewpoint of human eyes during bimanual tasks. The Realsense provides RGB-D images at a resolution of 640×480 with a frame rate of 30 Hz. The extrinsics between the camera and right arm base-frame are calibrated using the `easy_handeye` package¹. Additionally, an ARUCO marker² attached to the UR5e’s end-effector is employed to aid in the calibration process.

¹https://github.com/IFL-CAMP/easy_handeye

²https://github.com/pal-robotics/aruco_ros

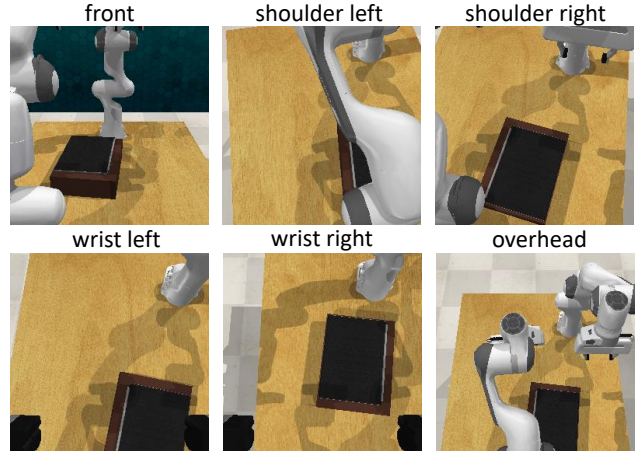


Figure 7. **Visual Observation in RLbench2.** We adopt 6 RGB-D cameras to cover the whole workspace.

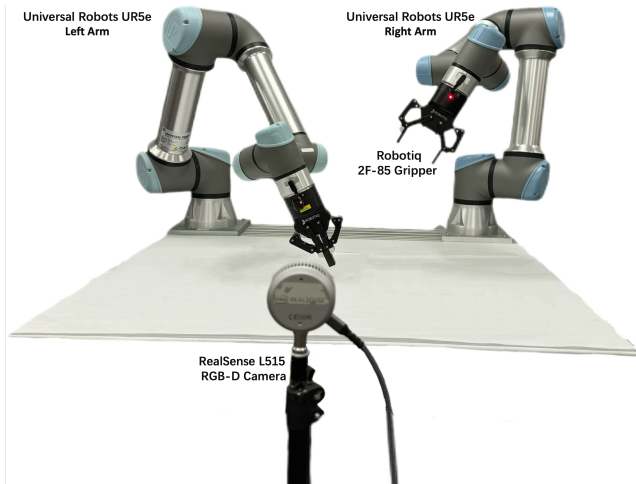


Figure 8. **Real-Robot Setup** with one RealSense L515 RGB-D Camera and Two UR5e Manipulators.

Tasksuite Descriptions. We provide a detailed description of the real-world tasks we used to evaluate our AnyBimanual in Figure 9, where we follow [42] to classify our 9 real-world experiments into 5 categories, covering 5 bimanual collaboration patterns.

- Lift Cabinet requires the agent to simultaneously hold two sides of the cabinet to lift it up, which poses challenges to synchronous coordination.
- Fold Clothes requires the agent to simultaneously grasp and fold the flexible clothes, which involves soft

Table 4. **Unimanual Tasks.** This table shows the 18 unimanual tasks in RLBench that are used to pretrain the unimanual policy.

Task	# of Variations	# of Average Keyframes	Human Instruction Template
open drawer	3	3.0	"open the ___ drawer"
slide block	4	4.7	"slide the block to ___ target"
sweep to dustpan	2	4.6	"sweep dirt to the ___ dustpan"
meat off grill	2	5.0	"take the ___ off the grill"
turn tap	2	2.0	"turn ___ tap"
put in drawer	3	12.0	"put the item in the ___ drawer"
close jar	20	6.0	"close the ___ jar"
drag stick	20	6.0	"use the stick to drag the cube onto the ___ target"
stack blocks	60	14.6	"stack ___ blocks"
screw bulb	20	7.0	"screw in the ___ light bulb"
put in safe	3	5.0	"put the money away in the safe on the ___ shelf"
place wine	3	5.0	"stack the wine bottle to the ___ of the rack"
put in cupboard	9	5.0	"put the ___ in the cupboard"
sort shape	5	5.0	"put the ___ in the shape sorter"
push buttons	50	3.8	"push the ___ button, [then the ___ button]"
insert peg	20	5.0	"put the ring on the ___ spoke"
stack cups	20	10.0	"stack the other cups on top of the ___ cup"
place cups	3	11.5	"place ___ cups on the cup holder"

Table 5. **Bimanual Tasks.** This table shows the 12 bimanual tasks in RLBench2 that are used to fine-tune the bimanual policy.

Task	# of Variations	# of Average Keyframes	Human Instruction Template
pick laptop	1	7.2	"pick up the notebook."
pick plate	1	6.6	"pick up the plate."
straighten rope	1	5.9	"straighten the rope."
lift ball	1	4.0	"lift the ball."
lift tray	1	5.1	"lift the tray."
push box	1	2.1	"push the box to the red area."
put in fridge	1	7.8	"put the bottle into the fridge."
press buttons	5	4.0	"push the ___ and ___ button."
handover item	5	7.6	"hand over the ___ item."
sweep to dustpan	1	7.3	"sweep the dust to the pan."
take out tray	1	8.7	"take tray out of oven."
handover easy	1	7.5	"hand over the item."

manipulation and synchronous coordination.

- **pick&place Sync** requires the agent to simultaneously pick up two colored cubes specified by the human instructions, and then place them in corresponding boxes, which involves semantic understanding.
- **Handover Bowl** requires the agent to lift a bowl and hand it over to the other hand, posing challenges in coordinating the handover between hands.
- **Wash Dishes** requires the agent to pick up a bowl and then apply detergent to it, testing the asynchronous coordination of both hands.
- **Play Ping Pong** requires the agent to pick up both a ball and a racket, toss the ball with one hand and hit it with the racket in the other in a high toss serve, testing asynchronous coordination.
- **Rotate Toothbrush** requires the agent to pick up a toothbrush and a cup simultaneously, then rotate the toothbrush 180 degrees to drop it into the cup, challenging the precision of rotation and coordination of both hands.
- **Type Writing** requires the agent to sequentially type the letters "robot" on a keyboard using both hands, testing long-horizon coordination.
- **Pick & Place Async** requires the agent to simultaneously pick up two cubes of different colors and then

place them into the same bowl, testing the asynchronous coordination of both hands.

Data Collection and Preprocessing. We collect demonstrations with two Xbox joysticks. Each gamepad is a 6-DoF controller. The gamepads adjust the velocity of the arm’s end-effector to translate and rotate in all directions, with reference to the arm’s base frame. For robot control, we utilize the Universal Robots ROS Driver³. After collecting the complete trajectory, we extract keyframes from the trajectory manually to simplify the robot learning. Two examples of the extracted keyframes are shown in Figure 10. The total time consumption of collecting one episode including controlling the robot arms and keyframe extraction is ~ 1.5 minutes.

Data Augmentation. In line with [31, 50], we turn on SE(3) augmentation to boost the robustness of all learned policies. Based on the open source code of [31], we modify the perturbation strategy to ensure that the perturbed ground-truth actions of both arms are reasonable in Figure 11. We plan to release our code for more details.

Policy Deployment. During the testing phase, we first randomize the positions of related objects in the current task.

³https://github.com/UniversalRobots/Universal_Robots_ROS_Driver

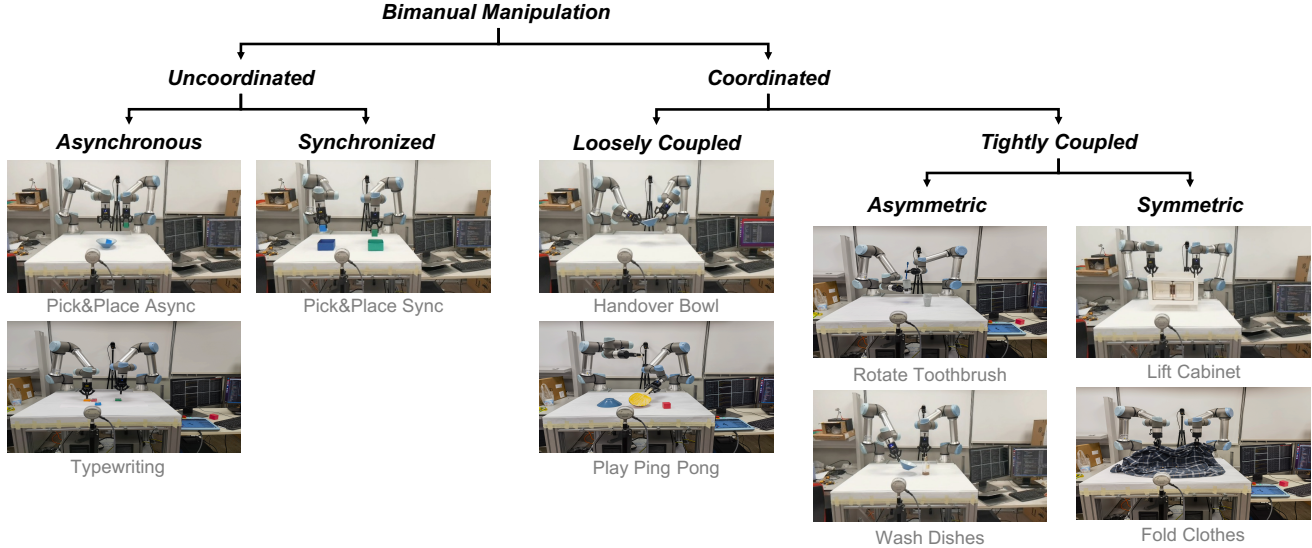


Figure 9. **Real-Robot Task Taxonomy.** Following [42], we classify the reported 9 real-world tasks into 5 categories according to their collaboration patterns.

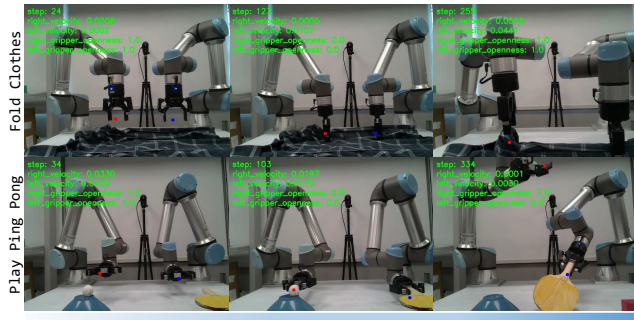


Figure 10. **Real-world Keyframes.** We manually select keyframes from the collected trajectories to simplify training.

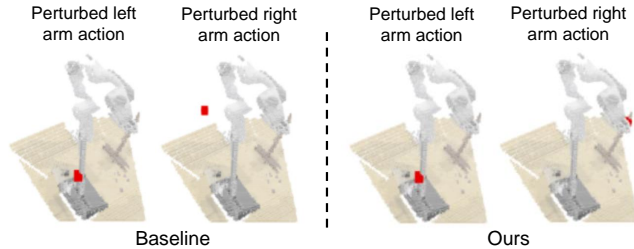


Figure 11. **SE(3) Augmentation.** We slightly modify the SE(3) augmentation strategy to ensure that the perturbed ground-truth actions of both arms are reasonable.

After resetting the manipulators to the home positions, we query the policy with the language instruction, initial observation and proprioception to obtain the next best poses of two end-effectors. We then use Moveit⁴ to reach the poses

⁴<https://github.com/moveit/moveit>

Table 6. **A default set of hyper-parameters.**

Config	Value
Training iteration	100k
Image size	$256 \times 256 \times 3$
Voxel size	$100 \times 100 \times 100$
Batch size	4
Optimizer	LAMB [67]
Learning rate	0.0005
Weight decay	0.000001
λ_{skill}	0.0001
λ_{voxel}	0.001
Number of skill primitives K	18
Dimension of Skill Representations D	512

and query the policy again with new observations, until task completion or reaching the maximal episode length.

7. Additional Implementation Details

7.1. Hyperparameters

The hyperparameters used in AnyBimanual are shown in Table 6. To ensure that the auxiliary objectives $\mathcal{L}_{\text{skill}}$ and $\mathcal{L}_{\text{voxel}}$ remain in the same magnitude as \mathcal{L}_{BC} , we set $\lambda_{\text{skill}} = 0.0001$ and $\lambda_{\text{voxel}} = 0.001$. Other hyperparameters are in line with previous works [31, 50] for fair comparisons.

7.2. Architectures

Skill Manager. We fuse voxel embeddings and language embeddings by projecting both to a hidden size of 256 and concatenating them. After layer normalization, the combined sequence is processed by a frozen GPT-2 Transformer configured with a hidden size of 256 and 8 attention heads. The transformer’s output is passed through a linear layer

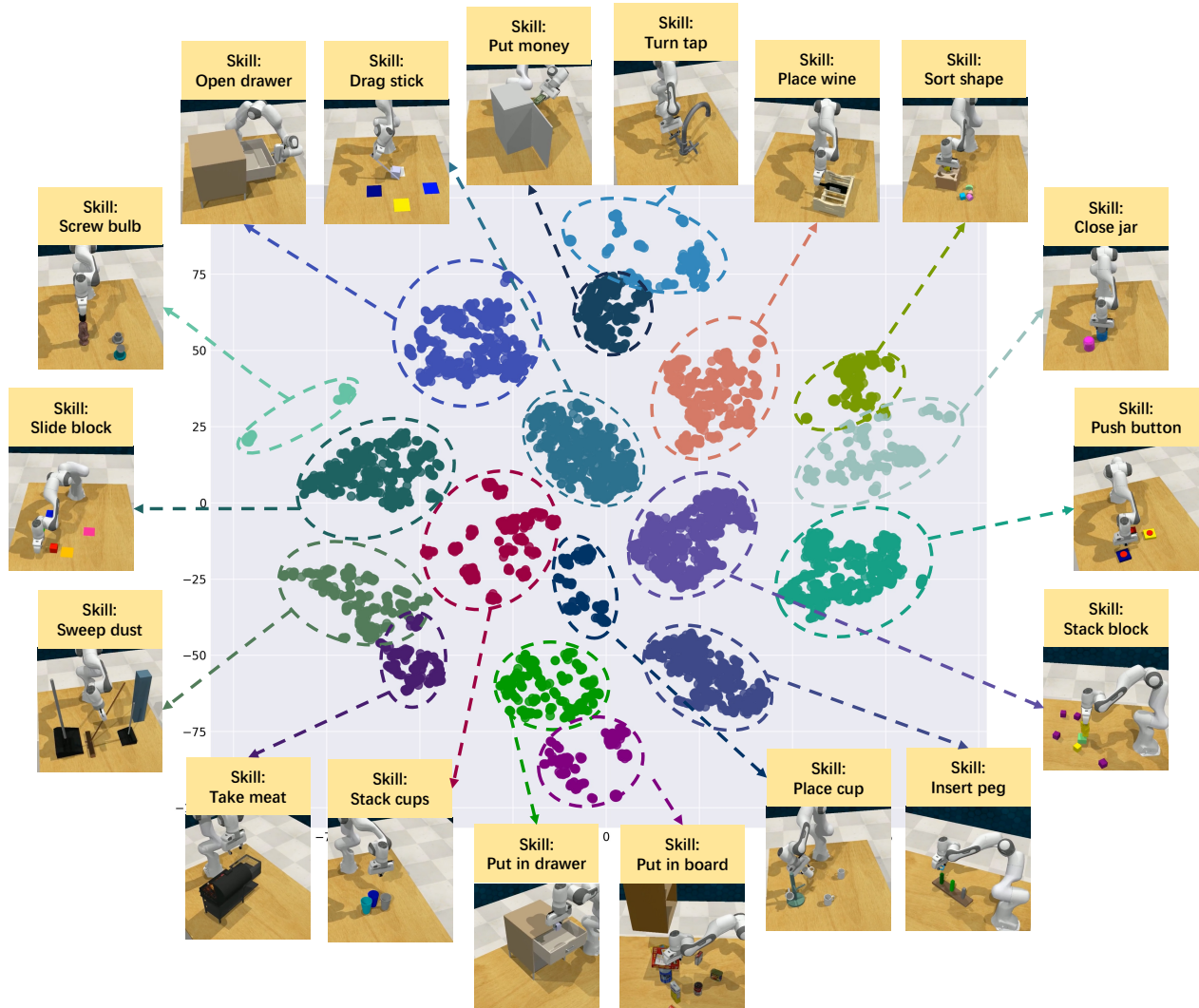


Figure 12. **Skill Clustering.** We cluster the skill representations to further interpret the discovered skills of our AnyBimanual.

to produce logits over 18 classes, and softmaxed to obtain probabilities. These probabilities are then used to reconstruct the skill representation via a weighted sum over the skill primitives.

Visual Aligner. We employ a lightweight module to process input embeddings through a Conv1D-ReLU block, then split into two branches to generate left and right masks via additional Conv1D-ReLU layers. After element-wise multiplication of these masks with the original input, we incorporate residual connections by adding the masked outputs back to the input embeddings.

7.3. Skill Primitives

The skill primitives use CLIP embeddings of unimanual language templates (*e.g.*, ‘open the ___ drawer’) from Table 1 of the supplementary file, as we expect them to represent foundational motions that generalize across object cat-

egories in unseen scenarios.

8. Additional Experimental Results

8.1. Skill Clustering

The goal of the skill manager is to obtain the language embedding via linear skill representations, so that the pre-trained unimanual policy model (*i.e.*, PerAct) can be prompted to generate feasible manipulation actions. In Figure 12, we cluster the skill representations while evaluating the last checkpoint of PerAct+AnyBimanual in RL-Bench2. We can observe that the learned skill representations are reasonably clustered into 18 categories, which corresponds to the number of pretrained unimanual tasks. We also visualize the related unimanual skill of each cluster by finding the nearest unimanual task embedding. The clustering results further interpret that the proposed skill manager en-

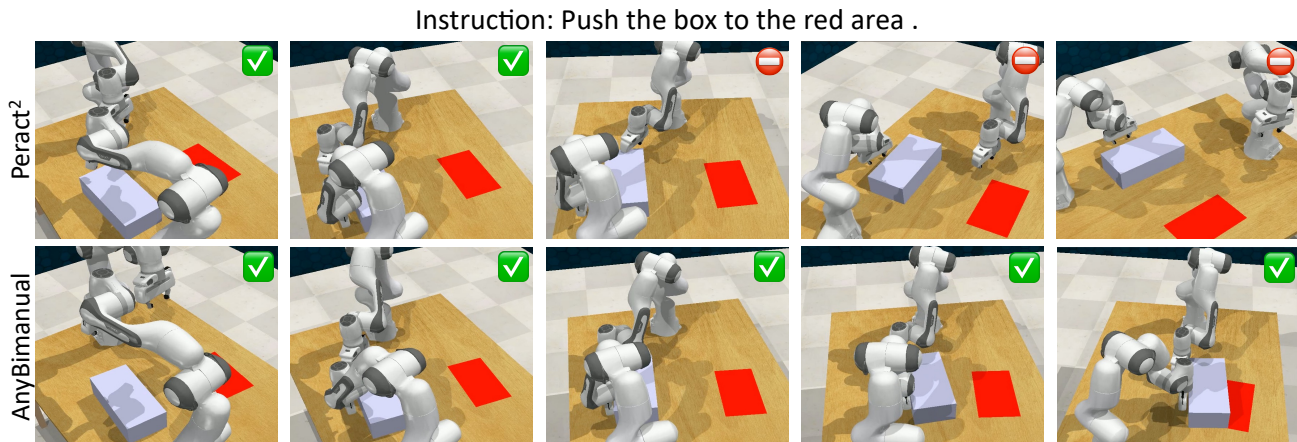


Figure 13. **Comparisons of the rollouts of PerAct² and our AnyBimanual.** AnyBimanual demonstrates complex collaboration patterns by incorporating the skill manager and the visual aligner to schedule the manipulators correctly.

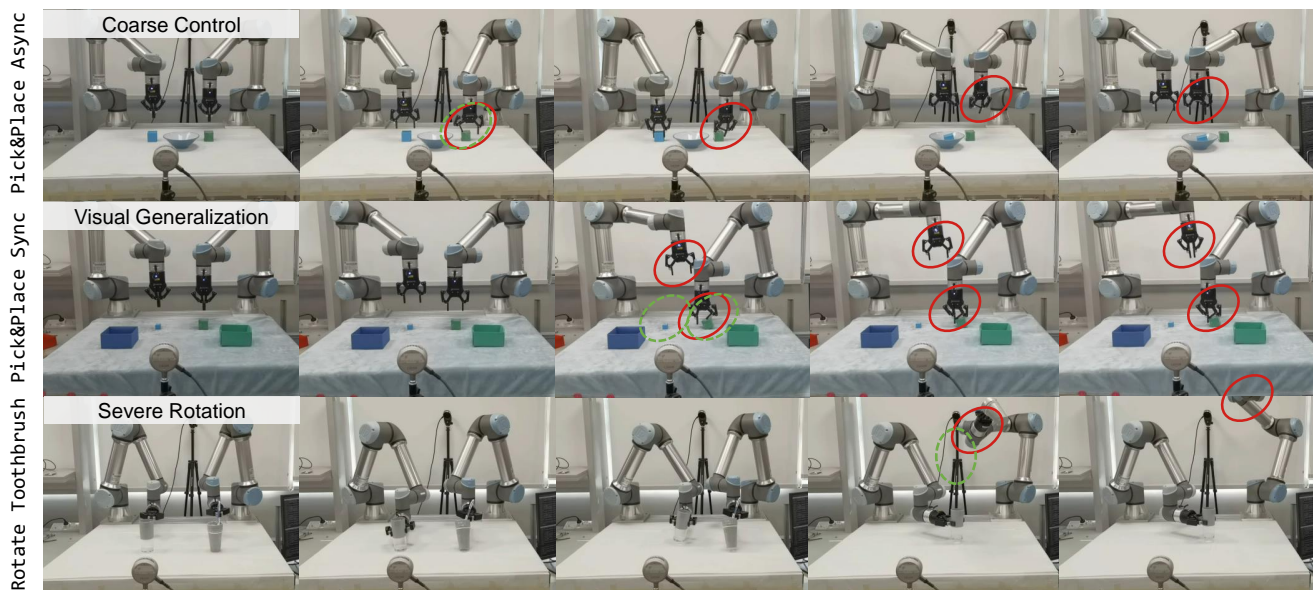


Figure 14. **Error Modes in Real-world Rollouts.** We study the common failure cases of our AnyBimanual in real-world settings, where the incorrect end-effector actions are marked with red circles. We also provide the correct actions with green circles for reference.

ables compact skill representation learning with rich semantics for dynamic scheduling.

8.2. Rollout Comparisons

We present a qualitative example of the generated action sequences in Figure 13, comparing PerAct² and our AnyBimanual method. In this case, the instruction is “Push the box to the red area”. The PerAct² agent fails to touch the box and only mimics the expert’s forward-pushing motion, resulting in an incomplete action. In contrast, our AnyBimanual agent ensures both arms make contact with the box and successfully push it into the red area, demonstrating the superior ability of our method in having each

arm correctly identify contact with the object and successfully complete the task.

8.3. Visualization

Skill Manager. We visualize the skill manager in two challenging tasks requiring heavy coordination. (Figure 15) AnyBimanual completes these tasks by scheduling skill representations across arms simultaneously and dynamically.

Visual Aligner. By predicting spatial soft masks for voxel observation, the visual aligner encourages both arms to focus on the interaction and ignore irrelevant parts. (Figure 16)

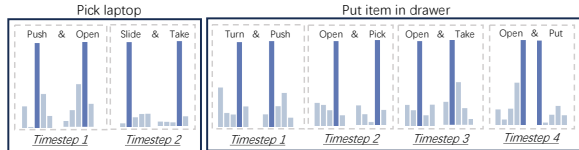


Figure 15. Visualization of Skill Manager.

8.4. Error Modes

To further study the limitations and risks of the proposed method, we visualize the common failure cases in Figure 14. Common error modes include coarse control, which is often viewed in *Pick&Place Sync* and *Pick&Place Async*. In the upper case, the robot fails to grasp the green block due to a small end-effector deviation, which may be caused by inconsistent data collection. In the middle case, the robot struggles to generalize to different backgrounds and object sizes, which leads to an out-of-distribution movement of the left robot arm. In the bottom case, the low-level motion planner cannot handle the severe rotation predicted by the agent, which can result in a dangerous cup fall. We hope that the analysis can enlighten future works in bimanual policy transferring and prevent potential risks in real-world deployments.



Figure 16. Visualization of Visual Aligner.

8.5. Bimanual Decomposability

We complement a heuristic measurement to assess the feasibility of decomposing a given bimanual task with a learned skill manager at the semantic level. Specifically, higher entropy in the predicted combination weights indicates greater difficulty in decomposition with certain unimanual primitives. In Figure 17, this metric strongly correlates with final success rates in four simulation tasks, delineating the boundary.

8.6. Real-world Videos

We provide 9 additional comprehensive real-world episodes generated by our AnyBimanual in the attached video file (*demo.mp4*). Note that all 9 tasks are completed by a single model with different natural language instructions to specify the current task.

8.7. Real-world Experiments with Limited Data.

To further validate the effectiveness and practicality of AnyBimanual with limited expert data, we train

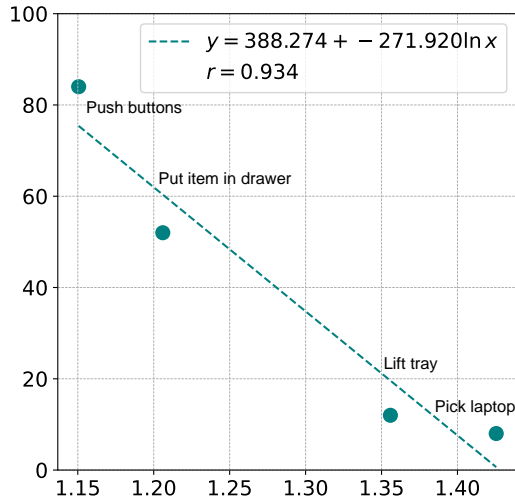


Figure 17. Bimanual Decomposability.

Table 7. Real-world Results with 5 Demonstrations Per Task. We train AnyBimanual on 9 real-world tasks with 5 demonstrations for each task, and evaluate each variation over 5 episodes.

Task	Success Rate (%)
Lift Cabinet	80.0
Fold Clothes	80.0
Pick&Place Sync	80.0
Handover Bowl	20.0
Wash Dishes	20.0
Play Ping Pong	40.0
Rotate Toothbrush	20.0
Typewriting	60.0
Pick&Place Async	80.0

AnyBimanual on 9 real-world tasks, each with 5 demonstrations. As per the main paper, we evaluate each variation over 5 episodes, and report the success rates of each task. The results are illustrated in Table 7, where AnyBimanual still maintains an acceptable average success rate of 53.33%.

9. Discussions on Limitations

Cross-embodiment Skill Transferring. AnyBimanual needs careful visual alignment between unimanual and bimanual systems to ensure robust policy transfer, which means it is not designed for cross-embodiment skill transferring. Even though the 7-DoF end-effector action space can be used with various robots, differences in the visual appearance of unimanual and bimanual robots may limit generalizability. Because the visual aligner only attempts to align the observation by segmenting out unimanual workspace from the bimanual system, without considering their appearance differences. This can be addressed by visual inpainting [59] or transferring cross-embodiment unimanual policies [58].

Cross-task Generalization. Although AnyBimanual enables general multi-task bimanual manipulation with few demonstrations, it struggles to perform zero-shot generalization to unseen tasks. This is mainly due to the end-to-end skill manager and visual aligner still necessitating expert demonstrations to learn proper coordination patterns and unlock the capacity of unimanual policy. Explicit methods such as leveraging large language models [25] to orchestrate unimanual policies can realize weak zero-shot generalization, but struggle with contact-rich tasks without learning.